Rigorous and Numerically Efficient Computation of the Irrotational Electric and Magnetic Eigenfunctions of Complex Gyrotron Cavities

Andreas Jöstingmeier, Christian Rieckmann, and A. S. Omar, *Senior Member, IEEE*

***Abstract*—For the modal analysis of complex gyrotron cavities, complete sets of eigenfunctions of the corresponding completely shielded cavity are required. In this contribution, it is shown that the generalized scattering matrix method which is well-known for the computation of the resonance modes can also be applied to the calculation of the irrotational electric and magnetic eigenfunctions. The irrotational eigenfunctions are computed for some circularly symmetrical structures. The validity of the method is checked by investigating a spherical cavity for which the analytical solution is known. Furthermore, a special subdivision of tapered cavity sections is presented which considerably improves the numerical efficiency of the method. For a standard gyrotron cavity, the field in the source region is computed with and without making use of irrotational electric eigenfunctions. It is demonstrated that the accuracy and the numerical efficiency of the modal expansion of the cavity field in the source region is improved if these eigenfunctions are included in the analysis.**

I. Introduction

In A gyrotron, the interaction between the electron beam and the electromagnetic field takes place in a rotationally symmetrical open cavity resonator. Nowadays, complex cavities which consist of cascaded line sections, steps, and tapers, see Fig. 1, are mostly used ([1], [2]). To simulate the operation of a gyrotron, an accurate representation of the electromagnetic field inside the cavity is required.

In [3] and [4], it has been demonstrated that for the modal expansion of the electromagnetic field inside open cavities the eigenfunctions of the corresponding completely shielded cavity can be used: By the application of the equivalence principle [5], the apertures of an open cavity can be short-circuited if the nonvanishing tangential electric field there is replaced by two surface magnetic currents at both sides of the short circuit, which are equal in magnitude and opposite in direction. Then, the electromagnetic field inside the cavity is expanded with respect to the complete set of the solenoidal *and* irrotational eigenfunctions of the corresponding completely shielded resonator [6].

Manuscript received February 11, 1994; revised July 27, 1994. This work was supported by the Deutsche Forschungsgemeinschaft.

A. Jöstingmeier and C. Rieckmann are with the Institut für Hochfrequenztechnik, Technische Universität Braunschweig, D-38023 Braunschweig, Germany.

A. S. Omar is with the Arbeitsbereich Hochfrequenztechnik, Technische Universität Hamburg-Harburg, D-21071 Hamburg, Germany.

IEEE Log Number 9410345.

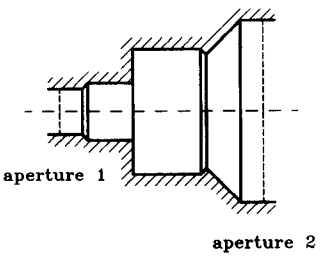

Fig. 1. Longitudinal section of a complex cavity.

One must keep in mind that the divergence-free resonance modes are not sufficient for the modal analysis. The irrotational magnetic eigenfunctions are mandatory due to the surface magnetic currents at the apertures of the cavity [7]. Consequently, the magnetic field is expanded in terms of the solenoidal magnetic eigenfunctions $\boldsymbol{H}_n$ which are the magnetic fields of the resonance modes *and* the irrotational magnetic eigenfunctions $\boldsymbol{G}_n$ which do not correspond to physical modes [6]

$$\boldsymbol{H} = \sum_n^\infty c_n \boldsymbol{H}_n + \sum_n^\infty d_n \boldsymbol{G}_n.$$

On the other hand, the electric field can either be expanded with respect to the solenoidal electric eigenfunctions $\boldsymbol{E}_n$ *and* the irrotational electric eigenfunctions $\boldsymbol{F}_n$

$$\boldsymbol{E} = \sum_n^\infty a_n \boldsymbol{E}_n + \sum_n^\infty b_n \boldsymbol{F}_n$$

or it can be written in terms of the solenoidal electric eigenfunctions only if $\boldsymbol{J}$ represents a well-behaved current density.

$$\boldsymbol{E} = \sum_n^\infty \bar{a}_n \boldsymbol{E}_n - \frac{\boldsymbol{J}}{j\omega\varepsilon_0}$$

(keeping in mind that the term $\boldsymbol{E} + \boldsymbol{J}/j\omega\varepsilon_0$ is divergence-free.) Note that the expansion coefficients a_n and $\bar{a}_n$ which correspond to the first and second expansion, respectively, have to be distinguished. Assuming that all solenoidal electric eigenfunctions $\boldsymbol{E}_n$ are normalized to the same energy W_0, i.e.,

$$\frac{\varepsilon_0}{2} \int_V |\boldsymbol{E}_n|^2 \, dV = W_0,$$

one arrives at

$$a_n \propto \frac{k_0^2}{k_n^2 - k_0^2} P_n,$$
$$\overline{a}_n \propto \frac{k_n^2}{k_n^2 - k_0^2} P_n,$$

where P_n which represents the excitation of the eigenfunction $\boldsymbol{E}_n$ by the electric current density $\boldsymbol{J}$ is given by

$$P_n = \int_V \boldsymbol{J} \cdot \boldsymbol{E}_n^* \, dV.$$

The quantities k_n and k_0 denote the resonance wavenumber of the nth solenoidal cavity mode and the free space wavenumber, respectively. For $k_n \gg k_0$, the expansion coefficients a_n and $\overline{a}_n$ are proportional to the terms $(k_0^2/k_n^2)P_n$ and P_n, respectively, which leads to a much faster convergence of the first expansion than that of the second one. Consequently, regarding accuracy and numerical efficiency the modal expansion in terms of the solenoidal electric eigenfunctions only is inferior to that with respect to the complete set of electric eigenfunctions. Only if very smooth current density distributions are considered for which the excitation integrals P_n decrease rapidly with increasing resonance wavenumbers k_n one would rather use the second expansion because it does not require the irrotational electric eigenfunctions.

Only for a few cavities the eigenfunctions can be derived analytically. Much work has already been done to calculate the resonance modes of a wide variety of structures. Usually, cavities which can be regarded as a waveguide with axially varying cross section can be subdivided into cascaded homogeneous waveguide sections which are separated by step discontinuities [8], [9]. For each individual step discontinuity the generalized scattering matrix [10] is computed by the application of, e.g., the mode-matching procedure. Subsequently, all scattering matrices are cascaded to obtain the overall scattering matrix. Short-circuiting the structure at two terminal planes leads to the resonance condition from which the resonance wavenumbers and the electromagnetic fields are determined.

In this contribution, this procedure which is well-known for the resonance modes is transferred to the determination of the irrotational eigenfunctions which can be derived in terms of a potential function satisfying the Helmholtz equation. Hence, the computation of these modes is to some extent similar to the calculation of the resonance modes. But one has to bear in mind that contrary to the resonance modes no magnetic (electric) field is related to the irrotational electric (magnetic) eigenfunctions. Furthermore, for the computation of the irrotational magnetic eigenfunctions, the so-called "TE_{00} waveguide mode" has to be taken into account. This mode is characterized by a transversely constant axial magnetic field only and is not included in the computation of the resonance modes.

A detailed discussion of the computation of the irrotational magnetic eigenfunctions in complex gyrotron cavities is given in [7]. Therefore, we concentrate on the irrotational electric eigenfunctions in this contribution. Although the computation of both types of irrotational eigenfunctions is similar to a certain extent one has to keep in mind that their roles in the analysis of open cavities clearly have to be distinguished.

In [7], it has been demonstrated that the irrotational magnetic eigenfunctions are mandatory for the modal analysis of open cavities if the eigenfunctions of the corresponding completely shielded cavity are used as expansion functions. To illustrate this, an analytic example has been discussed in detail in [7]. On the other hand, the irrotational electric eigenfunctions are not a must for the modal analysis. Nevertheless, it will be shown in this paper that in general the accuracy and the numerical efficiency of the modal expansion method can considerably be improved by including the irrotational electric eigenfunctions in the analysis. For this purpose, a cavity containing an electric current source is analyzed with and without making use of the electric eigenfunctions.

II. Theory

The irrotational electric eigenfunctions are defined by

$$\boldsymbol{F}_n = \nabla \varphi_n, \tag{1a}$$
$$\nabla^2 \varphi_n + p_n^2 \varphi_n = 0, \tag{1b}$$
$$\varphi_n = 0 \text{ on } S, \tag{1c}$$

where S and $\hat{\boldsymbol{n}}$ denote the surface of the completely shielded cavity and the outward directed unit vector normal to S, respectively. The quantities p_n are the eigenvalues of these modes. However, one has to keep in mind that these eigenvalues do not have the meaning of resonance frequencies because the irrotational eigenfunctions do not represent physical electric fields which satisfy the wave equations. They satisfy the boundary conditions only.

We concentrate on the analysis of a simple waveguide step as being the essential part of the whole structure, see Fig. 2. (Note that tapers can be seen as cascaded step discontinuities.) For $\varphi^{(\nu)}$ ($\nu = 1, 2$) we can use an expansion in terms of the corresponding waveguide modes. In the νth line section, the potential $\varphi^{(\nu)}$ corresponding to the eigenvalue p (the index n has been dropped) can then be written as

$$\varphi^{(\nu)} = \sum_i^{\infty} (c_i^{(\nu)+} e^{-j\beta_i^{(\nu)}(z-z_0)} + c_i^{(\nu)-} e^{+j\beta_i^{(\nu)}(z-z_0)}) \cdot \frac{k_i^{(\nu)}}{p} e_{zi}^{(\nu)}, \tag{2a}$$
$$(\beta_i^{(\nu)})^2 = p^2 - (k_i^{(\nu)})^2, \tag{2b}$$

where

$$c_i^{(\nu)+} = \begin{cases} a_i^{(\nu)} & \text{for } \nu = 1 \\ b_i^{(\nu)} & \text{for } \nu = 2 \end{cases}, \tag{2c}$$
$$c_i^{(\nu)-} = \begin{cases} b_i^{(\nu)} & \text{for } \nu = 1 \\ a_i^{(\nu)} & \text{for } \nu = 2 \end{cases}. \tag{2d}$$

The function $e_{zi}^{(\nu)}$ denotes the axial electric field of the ith TM mode in the νth waveguide and is defined by

$$\nabla_t^2 e_{zi}^{(\nu)} + (k_i^{(\nu)})^2 e_{zi}^{(\nu)} = 0, \tag{3a}$$
$$e_{zi}^{(\nu)} = 0 \text{ on the waveguide walls}, \tag{3b}$$

where ∇_t and $k_i^{(\nu)}$ are the transverse part of the del operator and the mode cutoff wavenumber, respectively. Equation (3b)

TABLE I
COMPARISON BETWEEN THE NORMALIZED EIGENVALUES OF SOME IRROTATIONAL ELECTRIC EIGENFUNCTIONS OF A SPHERICAL CAVITY THAT CORRESPOND TO THE THEORY OF SPHERICAL FUNCTIONS AND TO THE METHOD PRESENTED

Mode	F_{011}	F_{012}	F_{013}	F_{031}	F_{051}	F_{071}	F_{271}	F_{471}	F_{671}
Taper analysis	4.494	7.727	10.907	6.988	9.355	11.654	11.659	11.658	11.657
Exact value	4.493	7.725	10.904	6.988	9.356	11.657			

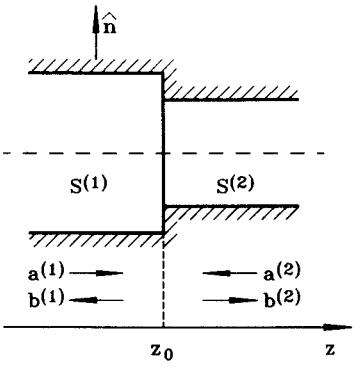

Fig. 2. Step discontinuity in a waveguide.

guarantees that the boundary condition (1c) is satisfied on the waveguide walls.

Matching the fields at both sides of the discontinuity yields

$$\varphi^{(1)} = \begin{cases} \varphi^{(2)} & \text{on } S^{(2)} \\ 0 & \text{on } S^{(1)} - S^{(2)} \end{cases}, \tag{4a}$$

$$\frac{\partial}{\partial z}\varphi^{(1)} = \frac{\partial}{\partial z}\varphi^{(2)} \text{ on } S^{(2)}. \tag{4b}$$

The continuity of both the potential and its normal derivative at $S^{(2)}$ is necessary in order to render the left-hand side of (1b) free from Dirac delta functions. Making use of the orthogonal properties of $e_{zn}^{(\nu)}$ [6], one gets

$$\boldsymbol{a}^{(2)} - \boldsymbol{b}^{(2)} = [A](\boldsymbol{a}^{(1)} - \boldsymbol{b}^{(1)}), \tag{5a}$$

$$\boldsymbol{a}^{(1)} + \boldsymbol{b}^{(1)} = [B](\boldsymbol{a}^{(2)} + \boldsymbol{b}^{(2)}), \tag{5b}$$

where the elements of the matrices $[B]$ and $[A]$ are given by the coupling integrals

$$B_{ij} = k_i^{(1)} k_j^{(2)} \int_{S^{(2)}} e_{zi}^{(1)} e_{zj}^{(2)}\, dS, \tag{5c}$$

$$A_{ji} = -\frac{\beta_i^{(1)}}{\beta_j^{(2)}} B_{ij}, \tag{5d}$$

respectively. The quantities $\boldsymbol{a}^{(\nu)}$ and $\boldsymbol{b}^{(\nu)}$ denote column vectors containing the expansion coeffficients $a_i^{(\nu)}$ and $b_i^{(\nu)}$, respectively. Equations (5a) and (5b) can be rearranged in scattering matrix notations, although we do not consider an ordinary scattering problem

$$\begin{bmatrix} \boldsymbol{b}^{(1)} \\ \boldsymbol{b}^{(2)} \end{bmatrix} = \begin{bmatrix} [S^{(11)}] & [S^{(12)}] \\ [S^{(21)}] & [S^{(22)}] \end{bmatrix} \begin{bmatrix} \boldsymbol{a}^{(1)} \\ \boldsymbol{a}^{(2)} \end{bmatrix}, \tag{6a}$$

where the submatrices $[S^{(\nu\mu)}]$ are given by

$$[S^{(22)}] = ([I] - [A][B])^{-1}([I] + [A][B]), \tag{6b}$$

$$[S^{(21)}] = -2([I] - [A][B])^{-1}[A], \tag{6c}$$

$$[S^{(12)}] = [B]([I] + [S^{(22)}]), \tag{6d}$$

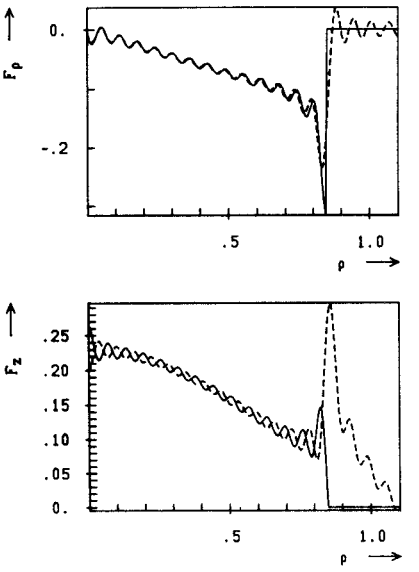

Fig. 3. Transverse and axial components of an irrotational electric eigenfunction at a waveguide step according to Fig. 2. The solid and the dashed lines correspond to waveguide 1 and 2, respectively.

$$[S^{(11)}] = -([I] - [B])[S^{(21)}]. \tag{6e}$$

If we consider now a complex structure composed of a number of line sections separated by step discontinuities, the scattering matrices corresponding to the different parts of the structure can be cascaded resulting in the overall scattering matrix of the whole structure which is denoted by $[\overline{S}]$. The application of the boundary condition

$$\boldsymbol{b}^{(\nu)} = -\boldsymbol{a}^{(\nu)} \tag{7}$$

at the short-circuited apertures $S^{(\nu)}$ (the terminal planes) leads to the "resonance condition"

$$\det([I] + [\overline{S}]) = 0. \tag{8}$$

From this relation, the eigenvalues p_n (and subsequently the field distribution) can be determined.

In [7], it has been shown that for the computation of the irrotational magnetic eigenfunctions the "TE_{00} waveguide mode" [11] has to be included. This mode corresponds to the constant term in a Fourier series. On the other hand, due to the boundary condition (3b) a "TM_{00} waveguide mode" does not exist. Note that this does not contradict the completeness of the set $\{e_{zi}^{(\nu)}\}$ because generally the $e_{zi}^{(\nu)}$ do not vanish in the mean.

III. NUMERICAL RESULTS

Computer codes for the calculation of irrotational eigenfunctions of complex circular waveguide cavities have been

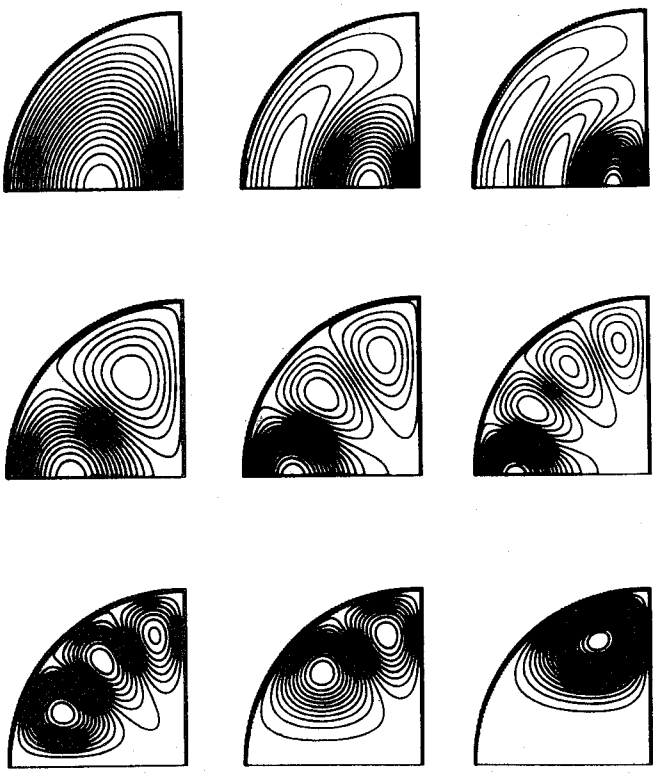

Fig. 4. Contour lines of the potentials which correspond to the irrotational electric eigenfunctions of a conducting hemisphere. The contour is approximated by five tapers.

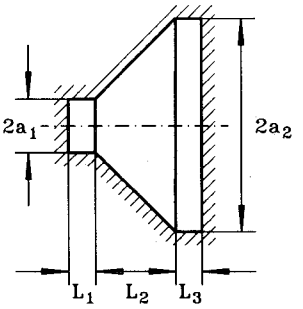

Fig. 5. Longitudinal section of a conical cavity.

developed. These codes can actually handle cavities which consist of cascaded line sections, step discontinuities and tapers. The number of steps into which each taper is subdivided, the spatial resolution which is given by the number of waveguide eigenfunctions, the number of evanescent modes which are taken into account for the interaction between adjacent steps, and the circumferential variations in the fields are input parameters. Output parameters are the eigenvalues and the contour lines of the potentials corresponding to the irrotational eigenfunctions.

In order to validate the numerical results the continuity of the transverse and the axial components of an irrotational electric eigenfunction is checked at a waveguide step. Fig. 3 presents the corresponding field distributions. Apart from the strong oscillations due to the field singularities at the 90° edge of the step [12], the field distributions corresponding to waveguide 1 (solid lines) and waveguide 2 (dashed lines) are

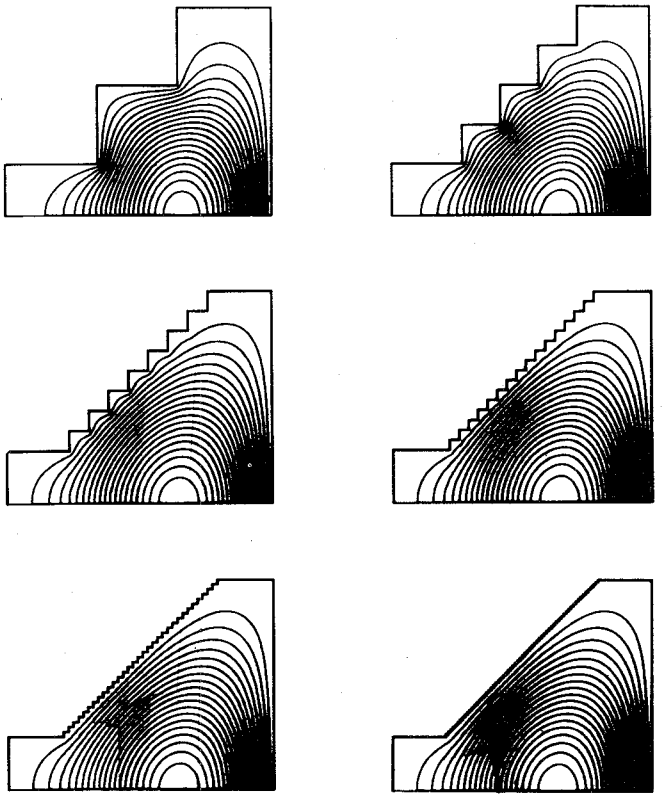

Fig. 6. Contour lines of the potentials which correspond to the azimuthally independent irrotational electric eigenfunctions with the lowest eigenvalues of a conical cavity according to Fig. 5. The taper is subdivided into 2, 4, 8, 16, 32, and 64 steps. Parameters: $a_1 = 1$ mm, $a_2 = 4$ mm, $L_1 = 1$ mm, $L_2 = 3$ mm, $L_3 = 1$ mm.

TABLE II
NORMALIZED EIGENVALUES OF THE EIGENFUNCTIONS ACCORDING TO FIG. 6

Number of steps	2	4	8	16	32	64
Eigenvalue	1.291	1.256	1.235	1.225	1.219	1.216
Relative cpu-time	0.022	0.056	0.120	0.248	0.493	1.000

well-matched throughout the common cross-section of both waveguides.

To subject the method to a further check a conducting hemisphere is investigated. The eigenvalues of this structure are identical to those of a spherical cavity which show electric wall symmetry in the equatorial plane. In Appendix A it is shown how the eigenvalues of the irrotational electric eigenfunctions of a conducting sphere are calculated using spherical functions. On the other hand, a sphere can be considered as a tapered circular waveguide. For a proper approximation of the contour, five tapers which are subdivided into apropiate numbers of steps are used. Tapers with different smoothnesses (i.e. number of steps per unit length) are necessary because of the wide range of taper slope characterizing a hemisphere as a taper. Near the poles, the slope is very small while near the equator it is very large. In Table I, the normalized eigenvalues of some spherical irrotational electric eigenfunctions are compared with the corresponding results of the taper analysis; and in Fig. 4 the contour lines of the corresponding potentials are given. The agreement between the results is excellent. Due to the rotational symmetry of the structure, it is sufficient to look

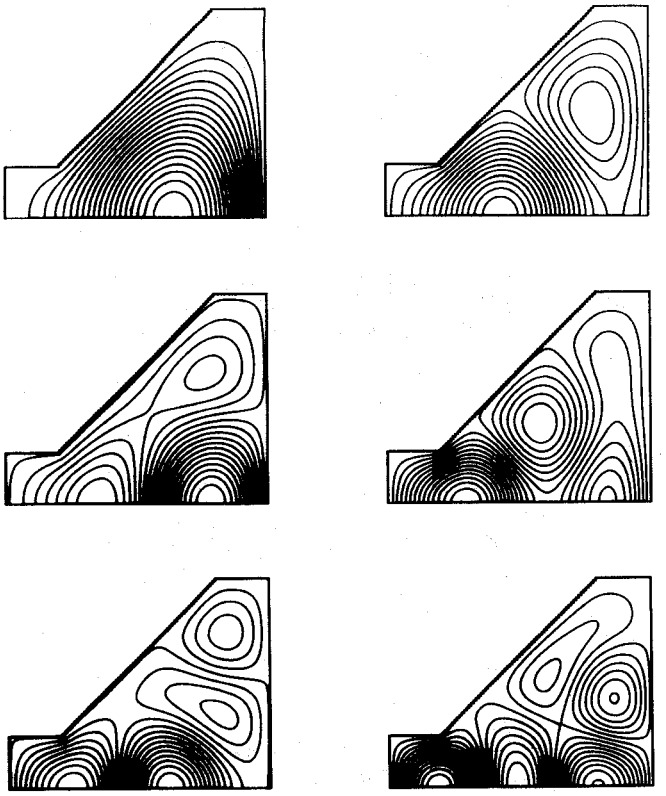

Fig. 7. Contour lines of the potentials that correspond to the azimuthally independent irrotational electric eigenfunctions with the six lowest eigenvalues of a conical cavity according to Fig. 5. The taper is subdivided into 64 steps. Parameters: as in Fig. 6.

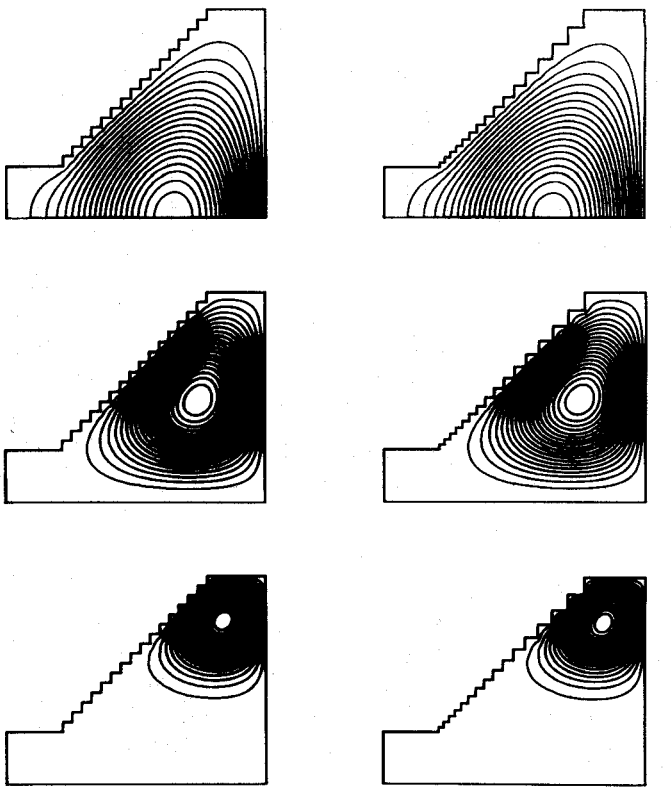

Fig. 8. Contour lines of the potentials that correspond to the irrotational electric eigenfunctions with the lowest eigenvalues of a conical cavity according to Fig. 5. The first, second, and third row of illustrations correspond to an azimuthal order of 0, 2, and 10, respectively, whereas the left and the right column correspond to the linear and the geometric subdivision of the taper (16 steps). Parameters: as in Fig. 6.

TABLE III
COMPARISON OF THE NORMALIZED EIGENVALUES AND CPU-TIMES THAT CORRESPOND TO THE LINEAR AND THE GEOMETRIC SUBDIVISION OF A CONICAL CAVITY ACCORDING TO FIG. 5. PARAMETERS: AS IN FIG. 6

Azimuthal order	Gender	Steps	Eigenvalue		Speed-up factor	Cpu-time in s
			Linear	Geometric		
0	F	2	1.291	1.303	1.7	2.4
		4	1.256	1.257	1.6	5.4
		8	1.235	1.235	1.6	12.6
		16	1.225	1.225	1.7	23.9
		32	1.219	1.219	1.7	48.1
		64	1.216	1.216	1.6	97.0
2	F	2	2.026	1.910	5.1	3.8
		4	1.961	1.980	6.1	6.8
		8	1.932	1.942	6.7	12.5
		16	1.916	1.922	6.8	24.5
		32	1.908	1.911	6.9	45.8
		64	1.903	1.905	6.9	90.3
10	F	2	4.039	3.897	8.6	4.9
		4	4.186	4.088	9.9	8.9
		8	4.166	4.179	10.1	17.5
		16	4.145	4.159	9.5	35.3
		32	4.133	4.141	9.2	70.6
		64	4.126	4.130	9.2	140.3

at its upper half. According to the boundary condition (1c), the contour lines have to be parallel to the boundary of the cavity. This is in good agreement with the plots. Although the contour lines give a good idea of the field structure, one has to keep in mind that they are not the field lines. The field lines are in fact normal to the contour lines everywhere.

Note that the taper analysis also yields the degeneracy of the $F_{071}, F_{271}, F_{471}$, and F_{671} modes, which is predicted by the theory of spherical functions.

Tapers are treated as cascaded steps, which may lead to huge computational requirements. Consequently, the number of steps should not be chosen larger than necessary. Fig. 5 shows the longitudinal section of a 45° conical cavity. For this structure, the influence of the number of steps into which the cone is subdivided on the eigenvalues, the field distributions, and the cpu-time is studied.

In Fig. 6 the contour lines of the potentials which correspond to the azimuthally independent irrotational electric eigenfunctions with the lowest eigenvalues for subdivisions of the cone into 2, 4, 8, 16, 32, and 64 steps are presented. Apart from the field in the immediate vicinity of the stepped boundary of the cone, the contour lines do not change significantly for subdivisions with more than 8 steps. This conclusion is confirmed by Table II in which the corresponding normalized eigenvalues and the relative cpu-times (the subdivision into 64 steps corresponds to 100%) are given. The difference between the eigenvalues which correspond to the subdivisions of the taper into 64 and 8 steps amounts only to 1.6%. On the other hand, the structure with 8 steps requires only 12% of the cpu-time needed for a subdivision of the taper into 64 steps.

For the expansion of the electromagnetic field with respect to a complete set of eigenfunctions, one has to compute quite a large number of irrotational electric eigenfunctions up to a

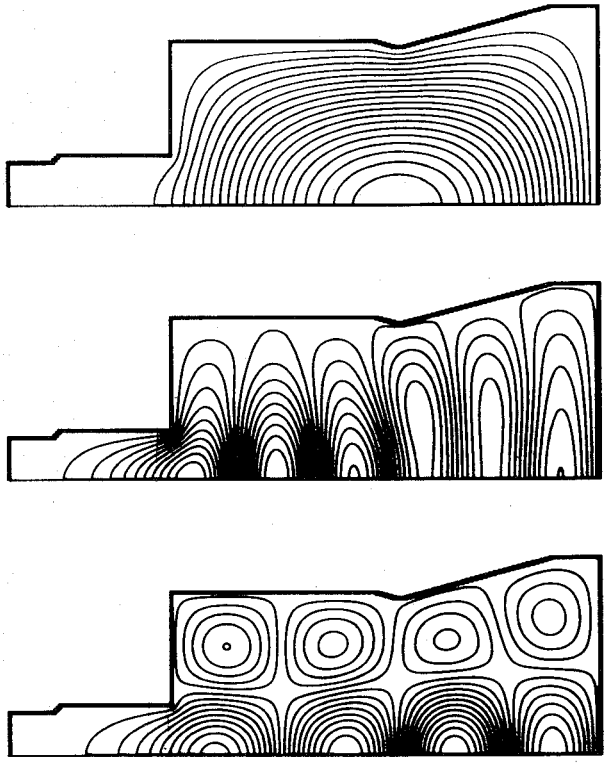

Fig. 9. Contour lines of the potentials that correspond to some azimuthally independent irrotational electric eigenfunctions of a complex gyrotron cavity.

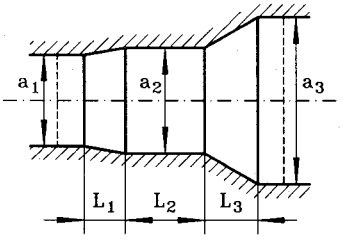

Fig. 10. Longitudinal section of a standard gyrotron cavity.

certain maximum eigenvalue p_n. Fig. 7 shows the contour lines of the potentials corresponding to the azimuthally independent irrotational electric eigenfunctions with the 6 lowest eigenvalues of the conical cavity shown in Fig. 5. Since only the first 6 eigenfunctions are calculated one can afford to subdivide the taper into 64 steps. Nevertheless, the computation of a whole set of eigenfunctions takes a lot of numerical efforts even if the number of steps is reduced. Therefore a considerable enhancement of the numerical efficiency of the method is discussed in the following.

In Appendix B it is shown that in a circular waveguide system, the coupling matrix $[B]$ of (5c) is a function of the ratio of the radii at both sides of a circular waveguide step only. Hence if a taper is subdivided such that this ratio is kept constant the same coupling matrix can be used for all steps which drastically reduces the computational requirements of the method [13]. This kind of subdivision is called geometric subdivision in contrast to a subdivision with equidistant steps which is denoted by linear subdivision. In Table III and in Fig. 8, the two subdivisions are compared for the conical cavity of Fig. 5. The eigenvalues corresponding to both subdivisions converge to each other.

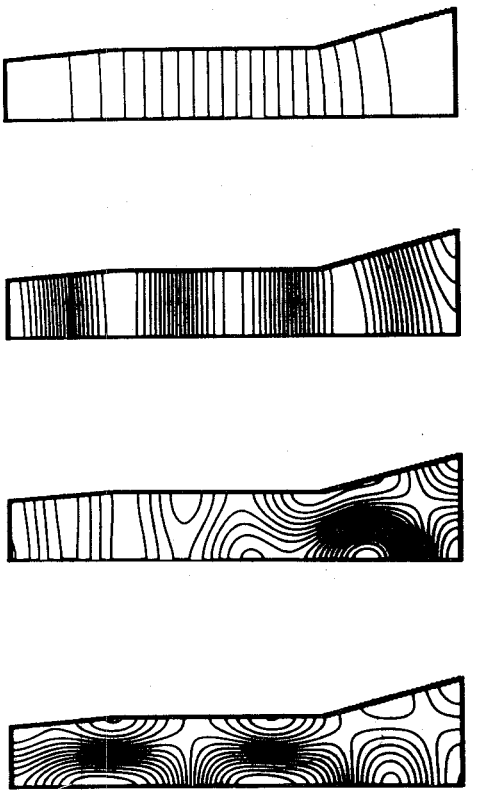

Fig. 11. Contour lines of the potentials that correspond to some azimuthally independent irrotational magnetic eigenfunctions of the standard gyrotron cavity shown in Fig. 10.

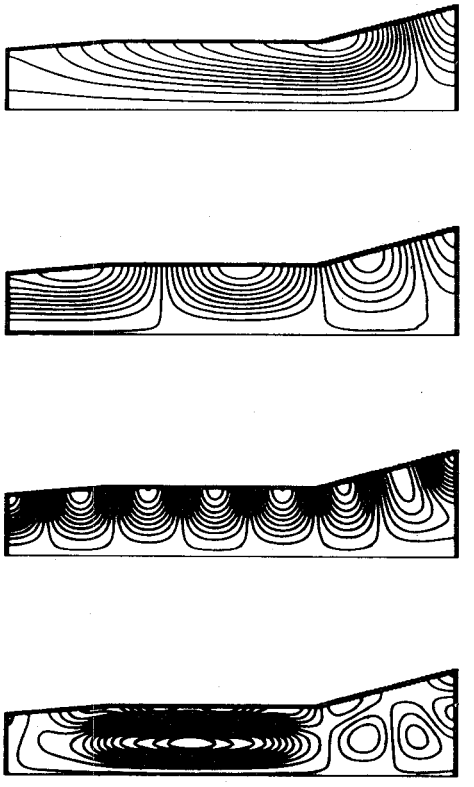

Fig. 12. Contour lines of the potentials that correspond to some irrotational magnetic eigenfunctions of the standard gyrotron cavity shown in Fig. 10, which show a second order azimuthal field variation.

The speed-up factor is defined as the ratio of the cpu-times required by the two subdivisions. For azimuthally independent

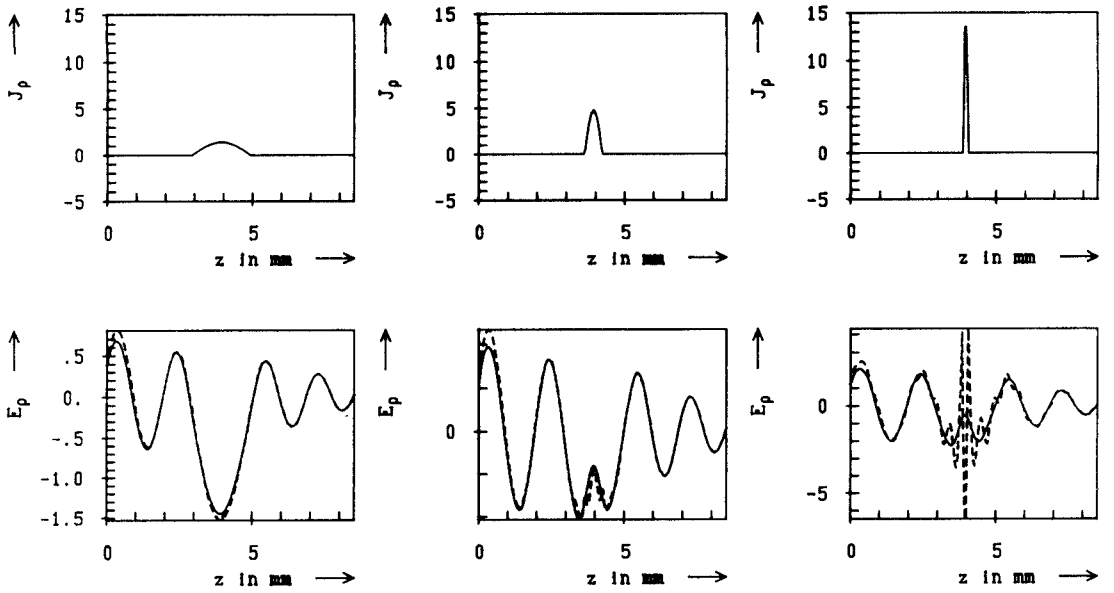

Fig. 13. Profiles of the transverse component of the electric field and the corresponding electric current density along the axis of a standard gyrotron cavity according to Fig. 10. The solid and the dashed lines correspond to modal expansions with and without irrotational electric eigenfunctions, respectively. Parameters: $a_1 = 1.74$ mm, $a_2 = 2$ mm, $a_3 = 1.54$ mm, $L_1 = 1.5$ mm, $L_2 = 3$ mm, $L_3 = 2$ mm, $f = 191$ GHz.

fields, the speed-up factor amounts only to about 1.7. This can be explained by the fast computation of the zero'th order Bessel functions so that the computation of the coupling matrices takes only little time. On the other hand, if higher order circumferential field variations are considered the speed-up factor increases significantly, it is about 10 for eigenfunctions with an azimuthal order of 10, which can be put down to the computation of the higher order Bessel functions because these functions are implemented as recurrence formulas. This feature makes the geometric subdivision especially attractive for whispering gallery fields which have recently been suggested for gyrotron operation.

The absolute cpu-times which are necessary for the computation of one eigenfunction assuming that the tapered section is geometrically subdivided are also given in Table III. The computer code has been implemented on a Convex C3840 vector computer, where vectorized NAG routines are used as far as possible. The computation of one eigenfunction of a cavity which is subdivided into 64 steps, which in general may belong to different tapers, requires about 2 minutes cpu-time. In a field expansion method, typically 100 eigenfunctions are needed which amounts to a total cpu-time of 200 minutes, which is quite high. But one has to keep in mind that once these eigenfunctions are computed for a cavity they can be stored and may serve as expansion functions for many applications.

Three azimuthally independent irrotational electric eigenfunctions of the complex gyrotron cavity shown in Fig. 1 are presented in Fig. 9. The cavity consists of one step discontinuity and three tapered sections which are subdivided into 3, 5, and 32 steps. The computation of each of the eigenfunctions takes about 1 minute cpu-time.

In Figs. 11 and 12, the contour lines of the potentials corresponding to some irrotational magnetic eigenfunctions of the standard gyrotron cavity shown in Fig. 10 are presented. The eigenfunctions shown in Fig. 11 are azimuthally independent whereas a second order azimuthal field variation is assumed in Fig. 12. The tapered sections are geometrically subdivided into 24 and 32 steps. According to the boundary condition for irrotational magnetic eigenfunctions [7], the contour lines have to be orthogonal to the boundary of the cavity which is in good agreement with the plots. Note that the contour lines of the eigenfunctions presented in the first two plots of Fig. [11] are approximately vertical. Consequently, the axial magnetic field is approximately constant throughout the cross section of the cavity. This illustrates that it is necessary to take the "TE_{00} waveguide mode" into account in each individual line section.

Finally, the modal expansions with and without irrotational electric eigenfunctions are compared for the standard gyrotron cavity which is excited by an impressed electric current density. For the sake of simplicity, it is assumed that the current density is given by an azimuthally independent radial component J_ρ only. In this case, an azimuthally independent TM field is excited. In the transverse direction, the current density distribution is assumed to be proportional to a Gaussian distribution with a standard deviation of 30% of the diameter a_2; whereas the corresponding axial dependence is given by a half sine wave. According to Fig. 13, three cases with different lengthes of the current density distributions are investigated. In all cases, the amplitude of the current density is chosen so that the total current is kept constant.

Fig. 13 also presents the distributions of the transverse component of the electric field E_ρ along the axis of the cavity, which correspond to the three current density distributions. The solid and the dashed lines correspond to the modal expansions with and without the irrotational electric eigenfunctions, respectively. Both expansions are carried out with the same spatial resolution. For a smooth current density distribution, as in the first case of Fig. 13, the agreement between the two expansions is excellent. On the other hand, as the current density distribution becomes more impulsive (as presented in

the second and third case of Fig. 13) the expansion without irrotational electric eigenfunctions is characterized by strong oscillations in the vicinity of the source (Gibbs phenomenon) whereas the expansion including these eigenfunctions is still well-behaved.

IV. Conclusion

The irrotational electric and magnetic eigenfunctions of complex cavities have been calculated based on the subdivision of the structure into cascaded step discontinuities. In a circular waveguide system, it has been demonstrated that the geometric subdivision of taper sections leads to a numerically efficient formulation. For several cavities, numerical results have been presented. The validity of the computer code has been illustrated for a spherical cavity. Moreover, it has been shown for a standard gyrotron cavity that the accuracy and the numerical efficiency of the modal expansion of the cavity field is improved by including the irrotational electric eigenfunctions in the analysis.

Appendix A

The resonance modes of a spherical cavity are well-known [5]. Modes which are either TE or TM to the radial coordinate r can be derived from the radial component ξ_{mnq} of an electric or magnetic vector potential, respectively, which is given by

$$\xi_{mnq} = \hat{J}_n(k_{nq}r)P_n^m(\cos\vartheta)\begin{Bmatrix}\cos(m\varphi)\\ \sin(m\varphi)\end{Bmatrix} \tag{A1}$$

where $\hat{J}_n(kr)$ and $P_n^m(\cos\vartheta)$ denote the spherical Bessel function according to

$$\hat{J}_n(k_{nq}r) = \sqrt{\frac{\pi k_{nq}r}{2}}J_{n+(1/2)}(k_{nq}r) \tag{A2}$$

and the associated Legendre function of the first kind. The quantity k_{nq} is the resonance wavenumber. The radial component of both, the electric and the magnetic vector potential satisfy the differential equation

$$(\nabla^2 + k_{nq}^2)\frac{\xi_{mnq}}{r} = 0. \tag{A3}$$

Since the potential φ_{mnq} corresponding to an irrotational electric eigenfunction fulfills the Helmholtz equation, φ_{mnq} and ξ_{mnq} are related by

$$\varphi_{mnq} = \frac{\xi_{mnq}}{r}. \tag{A4}$$

Due to the boundary condition (1c), the eigenvalues p_{nq} of φ_{mnq} are given by the characteristic equation

$$\hat{J}_n(p_{nq}a) = 0 \tag{A5}$$

where a denotes the radius of the conducting sphere. Note that the eigenvalues of a conducting sphere are identical to those of the resonance modes which are TE to r. In [5], some normalized eigenvalues $q_{np}a$ are given. A corresponding statement for the irrotational magnetic eigenfunctions is however not valid. In [7], it is demonstrated that the eigenvalues of these eigenfunctions have to be distinguished from the resonance wavenumbers of modes which are TM to r.

Appendix B

The waveguide eigenfunctions $e_{zi}^{(\nu)}$ are orthonormalized according to

$$(k_i^{(\nu)})^2\int_{S^{(\nu)}} e_{zi}^{(\nu)}e_{zj}^{(\nu)}\,dS = \delta_{ij} \tag{B1}$$

which leads to

$$e_{zi}^{\{{}_s^c\}(\nu)} = N_i^{\{{}_s^c\}}J_{p_i}\left(\frac{\chi_{p_i,q_i}}{r^{(\nu)}}\rho\right)\begin{Bmatrix}-\sin(p_i\varphi)\\ \cos(p_i\varphi)\end{Bmatrix} \tag{B2}$$

in a circular waveguide system. The superscripts "c" and "s" distinguish the cosine and the sine polarized eigenfunctions (with respect to the azimuthal component of the transverse electric field), respectively. For $p_i = 0$, only the sine polarization exists. The quantity χ_{p_i,q_i} denotes the q_ith zero of J_{p_i} which is different from zero. The quantity $r^{(\nu)}$ represents the radius of the νth line section. Note that the normalizing factor $N_i^{\{{}_s^c\}}$ which is given by

$$N_i^{\{{}_s^c\}} = \sqrt{\frac{2}{\pi}}\frac{1}{\chi_{p_i,q_i}}\frac{1}{J'_{p_i}(\chi_{p_i,q_i})}\begin{Bmatrix}1-\delta_{p_i0}\\ \dfrac{1}{\sqrt{1+\delta_{p_i0}}}\end{Bmatrix} \tag{B3}$$

is not a function of $r^{(\nu)}$.

Since waveguide eigenfunctions with different azimuthal orders ($p_i \neq p_j$) are decoupled it is convenient to define $p = p_i = p_j$. Substituting (B2) into the coupling integral of (5c) yields

$$B_{ij}^{\{{}_s^c\}} = -\frac{N_i^{\{{}_s^c\}}N_j^{\{{}_s^c\}}\pi\dfrac{r^{(2)}}{r^{(1)}}\chi_{p,q_i}(\chi_{p,q_j})^2}{(\chi_{p,q_j})^2 - \left(\dfrac{r^{(2)}}{r^{(1)}}\right)^2(\chi_{p,q_i})^2}J_p\left(\chi_{p,q_i}\frac{r^{(2)}}{r^{(1)}}\right)$$
$$\cdot J'_p(\chi_{p,q_j})\begin{Bmatrix}(1-\delta_{p0})\\ (1+\delta_{p0})\end{Bmatrix}. \tag{B4}$$

The coupling integral is only a function of the ratio $r^{(2)}/r^{(1)}$. Hence the same coupling matrix $[B]$ can be used throughout a taper if the taper is subdivided so that the ratio of the radii at each step is kept constant. This kind of subdivision is denoted by geometric subdivision.

References

[1] E. Jensen and K. Schunemann, "Potentials of complex cavities for efficiency enhancement of gyrotrons," in *9th Int. Conf. Infrared and Millimeter Waves*, Takarazuka, Japan, 1984, pp. 288–289.

[2] O. Dumbrajs and E. Borie, "A complex cavity with mode conversion for gyrotrons," *Int. J. Electron.*, vol. 65, pp. 285–295, 1988.

[3] Y. Y. Tsai and A. S. Omar, "Field theoretical treatment of H-plane waveguide junctions with anisotropic medium," *IEEE Trans. Microwave Theory Tech.*, vol. MTT-41, pp. 274–281, 1993.

[4] A. Jostingmeier and A. S. Omar, "Analysis of inhomogeneously filled cavities coupled to waveguides using the VIE formulation," *IEEE Trans. Microwave Theory Tech.*, vol. MTT-41, pp. 1207–1214, 1993.

[5] R. F. Harrington, *Time-Harmonic Electromagnetic Fields*. New York: McGraw-Hill, 1961.

[6] R. E. Collin, *Foundations for Microwave Engineering*. New York: McGraw-Hill, 1966.

[7] A. Jöstingmeier, C. Rieckmann, and A. S. Omar, "Computation of the irrotational magnetic eigenfunctions belonging to complex cavities," *IEEE Trans. Microwave Theory Tech.*, vol. MTT-42, pp. 2285–2293, 1994.

[8] H. Flügel and E. Kühn, "Computer-aided analysis and design of circular waveguide tapers," *IEEE Trans. Microwave Theory Tech.*, vol. MTT-36, pp. 332–336, 1988.
[9] J. M. Neilson, P. E. Latham, M. Caplan, and W. G. Lawson, "Determination of the resonant frequencies in a complex cavity using the scattering matrix formulation," *IEEE Trans. Microwave Theory Tech.*, vol. MTT-37, pp. 1165–1169, 1989.
[10] T. Itoh, "Generalized scattering matrix technique," in *Numerical Techniques for Microwave and Millimeter-Wave Passive Structures*. New York: Wiley, 1989, pp. 622–636.
[11] A. S. Omar, A. Jöstingmeier, and C. Rieckmann, "Application of the GSD technique to the analysis of slot-coupled waveguides," *IEEE Trans. Microwave Theory Tech.*, vol. MTT-42, pp. 2139–2148, 1994.
[12] R. E. Collin, *Field Theory of Guided Waves*. New York: IEEE Press, 1991.
[13] A. Jöstingmeier, C. Rieckmann, and A. S. Omar, "Numerically efficient taper analysis with controlled resolution," in *Proc. IEEE MTT-S Symp.*, Atlanta, GA, 1993, pp. 995–996.

Andreas Jöstingmeier was born in Bielefeld, Germany, on May 25, 1961. He received the Dipl.-Ing. degree in electrical engineering from the Technische Universität Braunschweig, Germany, in 1987, and the Doktor-Ing. degree from the Technische Universität Hamburg-Harburg, Germany, in 1991.

From 1987–1991 he worked as a research assistant at the Technische Universität Hamburg-Harburg where he was involved in the investigation of dielectric resonators. Since 1991 he has been with the Institut für Hochfrequenztechnik at the Technische Universität Braunschweig as a research assistant. His current fields of research are concerned with numerical methods for microwave and millimeter-wave structures and high-power millimeter-wave tubes.

Christian Rieckmann was born in Hamburg, Germany, on May 16, 1968. He received the Dipl.-Ing. degree in electrical engineering from the Technische Universität Hamburg-Harburg, Germany, in 1993.

Since 1993 he has been with the Arbeitsbereich für Hochfrequenztechnik at the Technische Universität Hamburg-Harburg as a research assistant. His current fields of research are concerned electromagnetic field theory and high-power generation.

A. S. Omar (M'87–SM'89), for a photograph and biography,see p. 944 of the June 1991 issue of this TRANSACTIONS.